

Irreversible Dynamics of the Phase Boundary in $U(\text{Ru}_{0.96}\text{Rh}_{0.04})_2\text{Si}_2$ and Implications for Ordering

A. V. Silhanek,¹ M. Jaime,¹ N. Harrison,¹ V. R. Fanelli,² C. D. Batista,¹ H. Amitsuka,³ S. Nakatsuji,⁴ L. Balicas,⁴
K. H. Kim,¹ Z. Fisk,⁴ J. L. Sarrao,⁵ L. Civale,⁵ and J. A. Mydosh⁶

¹National High Magnetic Field Laboratory, Los Alamos National Laboratory, MS E536, Los Alamos, New Mexico 87545, USA

²Department of Physics and Astronomy, University of California, Irvine, California 92697-4575, USA

³Graduate School of Science, Hokkaido University, N10W8 Sapporo 060-0810, Japan

⁴National High Magnetic Field Laboratory, Florida State University, Tallahassee, Florida 32306, USA

⁵MST Division, Los Alamos National Laboratory, Los Alamos, New Mexico 87545, USA

⁶II Physikalisches Institut, Universität zu Köln, 50937 Köln, Germany

(Received 20 July 2005; published 5 April 2006)

We report measurements and analysis of the specific heat and magnetocaloric effect-induced temperature changes at the phase boundary into the single magnetic field-induced phase (phase II) of $U(\text{Ru}_{0.96}\text{Rh}_{0.04})_2\text{Si}_2$, which yield irreversible properties similar to those at the valence transition of $\text{Yb}_{1-x}\text{Y}_x\text{InCu}_4$. To explain these similarities, we propose a bootstrap mechanism by which lattice parameter changes caused by an electric quadrupolar order parameter within phase II become coupled to the $5f$ -electron hybridization, giving rise to a valence change at the transition.

DOI: [10.1103/PhysRevLett.96.136403](https://doi.org/10.1103/PhysRevLett.96.136403)

PACS numbers: 71.27.+a, 75.30.Mb, 75.30.Sg

The broken symmetry order parameter responsible for the large specific heat anomaly at $T_0 \sim 17$ K in URu_2Si_2 continues to be of interest owing to its elusive “hidden” nature [1,2]. While there has been no consensus on the appropriate theoretical description of the “hidden order” (HO) phase [3–12], the key properties of the Fermi liquid, upon which the HO parameter is manifested, can be understood. Comprehensive de Haas–van Alphen (dHvA) measurements [13] reveal heavy quasiparticles with Ising spin degrees of freedom [14], indicating that nearly localized $5f$ -electron degrees of freedom contribute to the Fermi liquid. Within an Anderson lattice scheme, hybridization causes the itinerant quasiparticles to acquire the spin and orbital degrees of freedom of the lowest lying crystal electric field $5f^2$ multiplet [15]. Here, it is a Γ_5 non-Kramers doublet [6], making the quasiparticles in URu_2Si_2 possess both electric quadrupole (EQ) and Ising spin degrees of freedom [14].

Given the survival of “ Γ_5 quasiparticles” deep within the HO phase I [13,14,16], one can further assert that this phase must be explained by an itinerant Γ_5 quasiparticle model. This could also be an important factor in making an itinerant EQ order parameter difficult to detect, as proposed for exotic itinerant models [7,8,11,12]. Since the HO parameter remains undetected, the existence of Γ_5 quasiparticles necessitates an alternative question: can itinerant EQ degrees of freedom order, and, if so, how might such ordering differ from the established local moment EQ systems such as UPd_3 [17]? Until such questions are addressed by microscopic theory, an alternative approach to exploring the question of EQ order is to tip the balance of the interactions in favor of local moment EQ order of the type seen in UPd_3 [6,17]. In URu_2Si_2 this might be achieved in two ways. One is by Rh doping, which shifts the spectral weight of the $5f$ electrons away from the

Fermi energy [18], weakening their hybridization. Rh doping also inhibits \mathbf{q} -dependent itinerant mechanisms (nesting) by smearing the states at the Fermi surface. The other is by applying a strong magnetic field H , which enhances the effect of local correlations near the metamagnetic transition (at $\mu_0 H_m \sim 37$ T), causing the effective Fermi temperature T^* to collapse [19]. The partial polarization of the f electrons induced by H also strongly favors the XY order [20] (of EQ “pseudospins” orthogonal to the c axis) over Ising-antiferromagnetic order [6].

In this Letter, we propose that the strain sensitivity of an EQ order parameter couples it to the degree of $5f$ -electron hybridization V_{fc} . The transition into phase II in $U(\text{Ru}_{0.96}\text{Rh}_{0.04})_2\text{Si}_2$ [21] (shown in Fig. 1) then acquires thermodynamic similarities to the valence transition of YbInCu_4 [22,23], evident in both the magnetocaloric effect (MCE) and specific heat $C_p(T)$ data. Should a more local EQ order [6,17] occur, the associated lattice parameter changes can alter V_{fc} , which determines the effective “Kondo temperature” through the valence state of the system [22–24].

The MCE is convenient for studying H -dependent phase boundaries [25]. The quasiadiabatic sample temperature T is recorded while H is swept rapidly. When an order-disorder transition is crossed, entropy conservation causes an abrupt change δT in T . Typical δT measurements for $U(\text{Ru}_{0.96}\text{Rh}_{0.04})_2\text{Si}_2$ are shown in Fig. 1(b). The sudden increase in $T(H)$ on the H up sweep (red line) at $\mu_0 H \sim 27$ T indicates the onset of order: i.e., T increases to conserve entropy. The system then relaxes through a known thermal link to equilibrium with the bath before the next phase boundary, exiting phase II, is encountered at $\mu_0 H \approx 38$ T. Now δT changes sign as the ordered phase is abandoned. δT is larger at the high H phase boundary, owing to the larger jump in magnetization [21]. The mag-

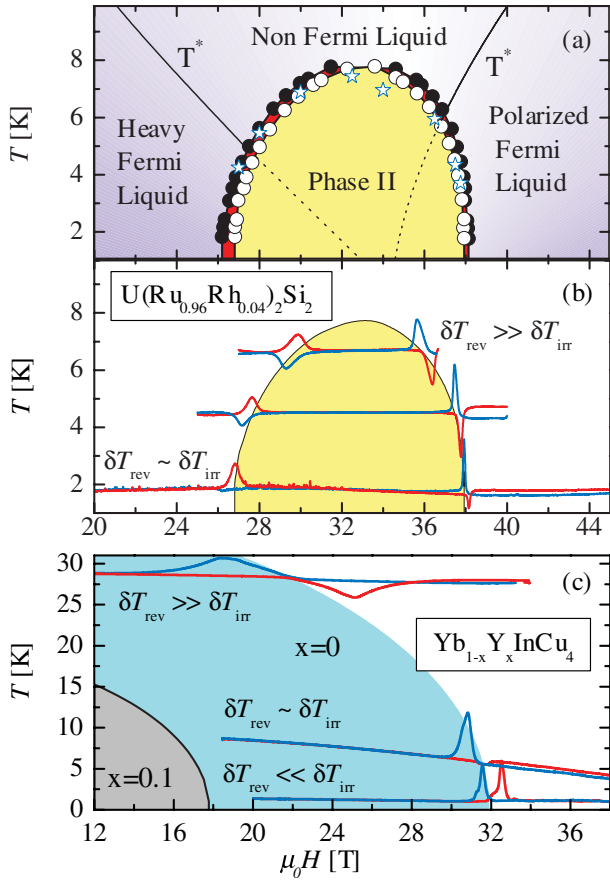


FIG. 1 (color). (a) Phase diagram of $U(Ru_{0.96}Rh_{0.04})_2Si_2$ determined by MCE (circles) and $C_p(T)$ (star symbols). Solid (open) circles indicate the phase boundary exiting (entering) the ordered phase II. The lines represent the approximate Fermi energy scale T^* , as modified by correlations due to metamagnetism [19]. (b) $\delta T(H)$ for $U(Ru_{0.96}Rh_{0.04})_2Si_2$ rescaled $\times 7$ ($\times 15$ at 2 K), with red (blue) indicating the rising (falling) field. (c) $\delta T(H)$ for $Yb_{1-x}Y_xInCu_4$, rescaled $\times 2$.

nitude of δT is also larger when entering phase II than exiting it. This behavior reveals a dissipative (irreversible) component δT_{irr} such that $\delta T = \delta T_{rev} + \delta T_{irr}$, indicating a 1st order transition.

While the combined MCE and thermal relaxation cause asymmetry of $\delta T(H)$, the magnitude of δT_{rev} retains the same value at a 2nd order transition, merely changing sign between rising and falling fields; i.e., it is reversible. Irreversible (or dissipative) processes at a 1st order transition, for example, due to the pinning of domain boundaries or metastability [26], introduce an additional δT_{irr} component that is always positive. Pinning forces become especially relevant if the order parameter involves charge degrees of freedom, as in valence transitions and EQ phases [6,23]. For a 1st order transition with both reversible and irreversible characteristics, the two components can be separated by taking the sum and difference between the total δT observed on rising and falling H . Figure 2 shows δT_{rev} and δT_{irr} for $U(Ru_{0.96}Rh_{0.04})_2Si_2$ and

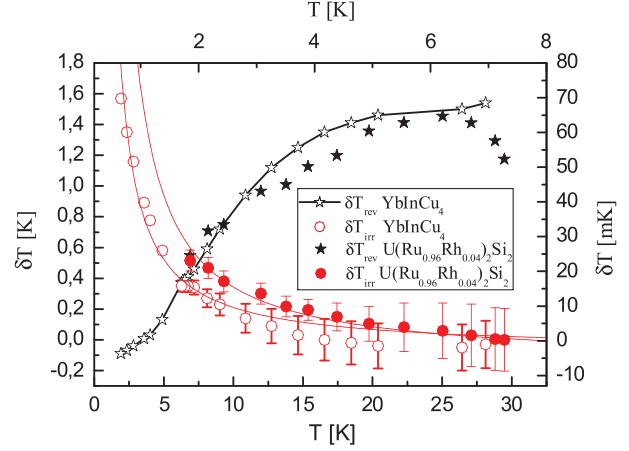


FIG. 2 (color). Irreversible δT_{irr} (circles) and reversible δT_{rev} (stars) MCE versus T for $U(Ru_{0.96}Rh_{0.04})_2Si_2$ (solid symbols) and $YbInCu_4$ (open symbols). The data corresponding to $U(Ru_{0.96}Rh_{0.04})_2Si_2$ ($YbInCu_4$) are linked to the right (left) and upper (lower) axes. Red lines are fits to $E_p(T)$ as described in the text, while the black line is to guide the eye.

$Yb_{1-x}Y_xInCu_4$ (with $x = 0$) thus extracted. In the case of $U(Ru_{0.96}Rh_{0.04})_2Si_2$, data is shown only for the lower critical field and the axes are rescaled for comparison. At higher T , δT_{rev} dominates the MCE in both materials, but the vanishing entropy causes δT_{rev} to vanish as $T \rightarrow 0$, whereupon δT_{irr} dominates. The latter grows rapidly as $T \rightarrow 0$, being especially clear in $YbInCu_4$ owing to the greater T range.

Similarities between $U(Ru_{0.96}Rh_{0.04})_2Si_2$ and $Yb_{1-x}Y_xInCu_4$ extend to $C_p(T)$. Figure 3 shows $C_p(T)$ for $U(Ru_{0.96}Rh_{0.04})_2Si_2$ and $Yb_{1-x}Y_xInCu_4$ (with $x = 0$ and 0.1) measured at constant H using the thermal relaxation time method [25] (both during warming and cooling using a small $\sim 1\% - 3\%T$ increment). The first $C_p(T)$ point measured at each T on warming yields a larger value (solid symbols) than subsequent points (open symbols), consistent with the irreversibilities observed using the MCE. However, unlike with the MCE, neither the first or subsequent points can be used to extract the precise entropy change at the transition. The former includes the energy absorbed by irreversible processes (depinning domain boundaries, etc.) in addition to the equilibrium $C_p(T)$. Once the sample has settled into a new metastable state at each T , subsequent measurements have a much reduced effect on its state, lowering the $C_p(T)$ estimate. Type-II superconductors are well known to give rise to a similar irreversible behavior [27].

It is, nevertheless, worth emphasizing the primary difference between $U(Ru_{0.96}Rh_{0.04})_2Si_2$ and $Yb_{1-x}Y_xInCu_4$. The valence instability in $Yb_{1-x}Y_xInCu_4$ is the consequence of multiple minima in its total free energy as a function of the volume and V_{fc} [22,23]. One can consider the mean value of the hybridization operator as the effective order parameter, although the f -electron density is the usual choice. Such an order parameter is nonsymmetry

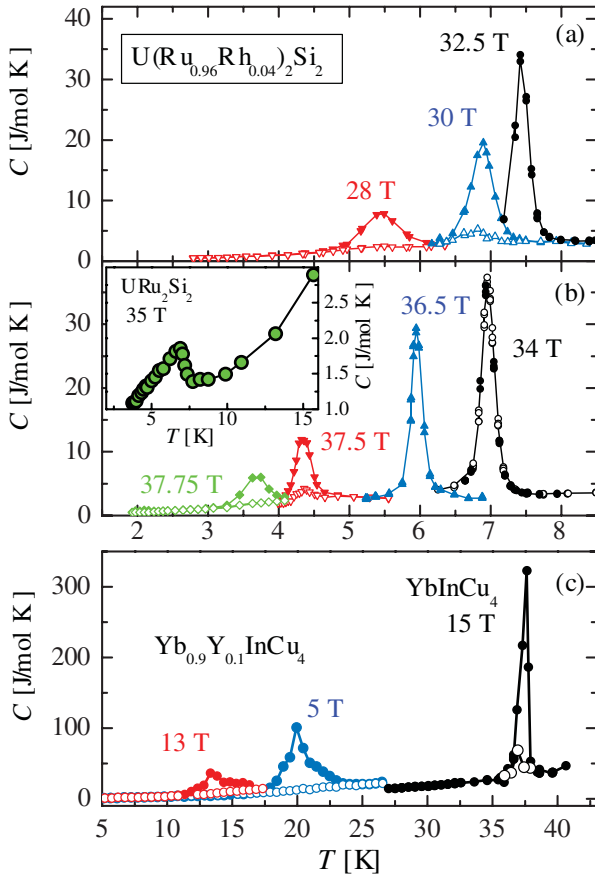


FIG. 3 (color). $C_p(T)$ at different values of H measured on (a) $\text{U}(\text{Ru}_{0.96}\text{Rh}_{0.04})_2\text{Si}_2$ for $\mu_0 H < 34$ T, (b) $\text{U}(\text{Ru}_{0.96}\text{Rh}_{0.04})_2\text{Si}_2$ for $\mu_0 H \geq 34$ T, and (c) $\text{Yb}_{1-x}\text{Y}_x\text{InCu}_4$ (with $x = 0.1$) using a superconducting magnet. Solid symbols represent C_p measured with the first heat pulse on warming up, while open symbols represent the average of subsequent heat pulses. The inset shows $C_p(T)$ for pure URu_2Si_2 at 36 T.

breaking, making it analogous to the boiling point of a liquid. However, unlike the valence instabilities in $\text{Yb}_{1-x}\text{Y}_x\text{InCu}_4$ and $\text{Ce}_{0.8}\text{Th}_{0.1}\text{La}_{0.1}$ [22–24], the transition into phase II is of 2nd order in pure URu_2Si_2 , as depicted in the inset to Fig. 3(b) [25,28], unambiguously establishing broken symmetry. It evolves into a large 1st order anomaly only as phase II grows to dominate the phase diagram on Rh doping [19,21]. Phase II in $\text{U}(\text{Ru}, \text{Rh})_2\text{Si}_2$ occurs also only under strong magnetic fields in a regime where the local $5f$ moments become liberated by the suppression of T^* (i.e., heavy Fermi liquid bandwidth) [19]. Since T^* becomes small compared to its transition temperature ($T_v \approx 7.8$ K) near H_m , the energy scale of the quasiparticles becomes irrelevant compared to the effective exchange interactions between the local Γ_5 pseudospin degrees of freedom. An effective antiferromagnetic exchange interaction prevents the Γ_5 moments from full alignment along H . A canted pseudospin phase results from the competition between H and the antiferromagnetic exchange. This corresponds to a large Z component (uniform magnetization) along H with a finite XY component

that orders according to the exchange interaction. A staggered EQ moment (XY component of the Γ_5 doublet) is then the most natural candidate for the order parameter of phase II. This scenario also explains why phase II is first induced and later suppressed as a function of H . Upon drawing an analogy with field-induced XY antiferromagnets [20], H_{c1} is then the critical field required to liberate the $5f$ moments, while H_{c2} is the field required to saturate the magnetization, reducing the XY component to zero. Such a broken symmetry order parameter, here involving a change in lattice parameters so as to change V_{fc} within phase II, would provide a rather effective bootstrap mechanism for both ensuring its stability and causing the transition to become 1st order like that in YbInCu_4 . A change in V_{fc} is implicit to the large changes in strain at high magnetic fields recently observed in pure URu_2Si_2 by Correa *et al.* [29].

Having established that the f -electron valence is strongly coupled to the thermodynamics of both $\text{U}(\text{Ru}_{0.96}\text{Rh}_{0.04})_2\text{Si}_2$ and $\text{Yb}_{1-x}\text{Y}_x\text{InCu}_4$, further analysis of the irreversible processes are required in order to understand Fig. 2. The increase in δT_{irr} as $T \rightarrow 0$ is consistent with the loss of thermal fluctuations, which would otherwise enable the domain boundaries to overcome pinning forces and undergo creep at finite T . Type II superconductors provide a good analogue for understanding creep [30], with the supercurrents sustained by pinned vortices being replaced in the present valence systems by the magnetic currents associated with the magnetization difference ΔM between domains. To model the present experimental data, we introduce a phenomenological model for the nonequilibrium energy $E_p(T) \propto \exp(U_0/k_B T) - \exp(U_0/k_B T_v)$ stored due to pinning. While it is ΔM that enables the system to store energy, it is ultimately the pinning force that limits the total storage capacity of the sample. In a thermal activation model, like that described above, the strength of the pinning is most conveniently parameterized in terms of a potential U_0 [30]. Here, we must also introduce a second constant term containing the optimum (maximum) transition temperature T_v to constrain the model so that $E_p(T)$ vanishes when $\Delta M \rightarrow 0$ and $T \rightarrow T_v$. $T_v \approx 7.8$ K at ≈ 34 T in $\text{U}(\text{Ru}_{0.96}\text{Rh}_{0.04})_2\text{Si}_2$ [see Fig. 4(a)] while $T_v \approx 40$ K at $H = 0$ in $\text{Yb}_{1-x}\text{Y}_x\text{InCu}_4$. On sweeping the magnetic field, $E_p(T, H)$ manifests itself as an irreversible (hysteretic) contribution to the magnetization δM_{irr} [31]. This energy is released as heat when the phase boundary is crossed, giving rise to the irreversible contribution δT_{irr} . Upon making a rather simple assumption that $\delta T_{\text{irr}}(T) \propto E_p(T)$, fits of $E_p(T)$ in Fig. 2 reproduce the experimental data rather well for $\text{U}(\text{Ru}_{0.96}\text{Rh}_{0.04})_2\text{Si}_2$ and $\text{Yb}_{1-x}\text{Y}_x\text{InCu}_4$, yielding $U_0 = 1.0 \pm 0.3$ K for both systems. Time-dependent magnetization measurements of $\text{Yb}_{1-x}\text{Y}_x\text{InCu}_4$ (with $x = 0.1$) in Fig. 4(b) provide rather direct evidence for metastability and creep, revealing that, after cooling the sample partway through the transition, the magnetization changes slowly under a constant H and T ,

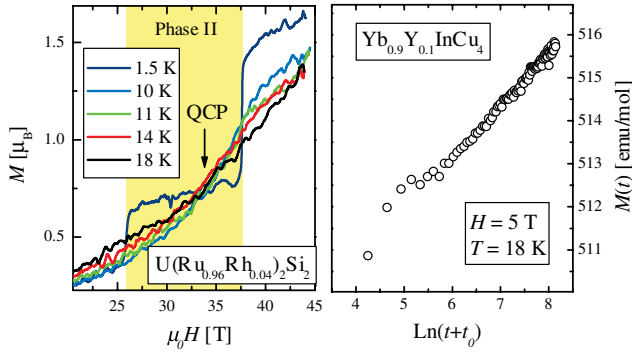


FIG. 4 (color). (a) Magnetization as a function of field at several temperatures for the $U(Ru_{0.96}Rh_{0.04})_2Si_2$ sample. (b) Relaxation of the magnetization for the $Yb_{0.9}Y_{0.1}InCu_4$ sample at $\mu_0 H = 5$ T and $T = 18$ K plotted as a stretched exponential.

having an approximate logarithmic time dependence. The large critical fields prevent an equivalent study from being made on $U(Ru_{0.96}Rh_{0.04})_2Si_2$.

In contrast to the MCE, the difference in $C_p(T)$ between the first and subsequent heat pulses presented in Fig. 3 cannot be utilized to extract $E_p(T)$. Nevertheless, the inability of $U(Ru_{0.96}Rh_{0.04})_2Si_2$ to store a significant non-equilibrium energy as $\Delta M \rightarrow 0$ at ≈ 34 T may account for the loss of irreversibility in $C_p(T)$ in Fig. 3(b) at that field.

In summary, we have shown that the irreversible properties of the transition into the field-induced phase (phase II) of $U(Ru_{0.96}Rh_{0.04})_2Si_2$ are very similar to that associated with the valence transition of $Yb_{1-x}Y_xInCu_4$. While the transition into phase II is of 2nd order in pure URu_2Si_2 , the combined effect of H and Rh-doping on T^* favors local moment ordering. This enables phase II to become much more efficient at minimizing the total free energy of the system compared to the other phases, therefore dominating the phase diagram in $U(Ru_{0.96}Rh_{0.04})_2Si_2$. On considering the local electric quadrupolar degrees of freedom of a lowest energy Γ_5 doublet [14], an antiferro-quadrupolar order parameter is the more natural choice. Such an order parameter is known to be sensitive to the effect of strain, which could then explain why it becomes strongly coupled to V_{fc} and the $5f$ valence. In contrast to the HO phase I, local moment ordering within phase II should lend itself more easily to the established local spectroscopic probes such as nuclear quadrupole resonance and resonant x-ray scattering [17].

The itinerant order parameter responsible for the low H HO phase I in pure URu_2Si_2 may instead lend itself more accessible to probes that are suitable for studying itinerant quasiparticles, such as the dHvA effect. Such probes have already revealed the Zeeman splitting of quasiparticles with Ising spin degrees of freedom [14], but should be extended to studying the equivalent splitting of EQ degrees

of freedom by applying uniaxial strain in the X or Y direction.

This work was performed under the auspices of the National Science Foundation, the Department of Energy (U.S.), and the state of Florida. J. A. M. is supported by the A. von Humboldt Foundation. V. R. F. acknowledges support of DOE funding.

- [1] K. Matsuda *et al.*, Phys. Rev. Lett. **87**, 087203 (2001).
- [2] K. Behnia *et al.*, Phys. Rev. Lett. **94**, 156405 (2005).
- [3] V.L. Libero and D.L. Cox, Phys. Rev. B **48**, 3783 (1993).
- [4] V. Barzykin and Gor'kov, Phys. Rev. Lett. **70**, 2479 (1993).
- [5] P. Santini and G. Amoretti, Phys. Rev. Lett. **73**, 1027 (1994).
- [6] F. Ohkawa, and H. Shimizu, J. Phys. Condens. Matter **11**, L519 (1999).
- [7] P. Chandra *et al.*, Nature (London) **417**, 831 (2002).
- [8] A. Virosztek, K. Maki, and B. Dora, Int. J. Mod. Phys. B **16**, 1667 (2002).
- [9] A. Kiss and P. Fazekas, Phys. Rev. B **71**, 054415 (2005).
- [10] V.P. Mineev and M.E. Zhitomirsky, Phys. Rev. B **72**, 014432 (2005).
- [11] C.M. Varma and L. Zhu, Phys. Rev. Lett. **96**, 036405 (2006).
- [12] V. Tripathi, P. Chandra, and P. Coleman, J. Phys. Condens. Matter **17**, 5285 (2005).
- [13] H. Ohkuni *et al.*, Philos. Mag. B **79**, 1045 (1999).
- [14] A. Silhanek *et al.*, cond-mat/0506384 [Physica B (Amsterdam) (to be published)].
- [15] J.G. Park *et al.*, Phys. Rev. B **66**, 094502 (2002).
- [16] Presumably true also for the Ising-antiferromagnetic phase observed under pressure, since the Fermi surface topology there is observed to be the same as for the HO phase; M. Nakashima *et al.*, Physica B (Amsterdam) **329**, 566 (2003).
- [17] D.F. McMorrow *et al.*, Phys. Rev. Lett. **87**, 057201 (2001).
- [18] L.M. Sandratskii and J. Kubler, Solid State Commun. **91**, 183 (1994).
- [19] A. Silhanek *et al.*, Phys. Rev. Lett. **95**, 026403 (2005).
- [20] M. Jaime *et al.*, Phys. Rev. Lett. **93**, 087203 (2004).
- [21] K.H. Kim *et al.*, Phys. Rev. Lett. **91**, 256401 (2003); K.H. Kim *et al.*, Phys. Rev. Lett. **93**, 206402 (2004).
- [22] C. Dallera *et al.*, Phys. Rev. Lett. **88**, 196403 (2002).
- [23] N.V. Mushnikov *et al.*, Physica B (Amsterdam) **334**, 54 (2003).
- [24] F. Drymiotis *et al.*, J. Phys. Condens. Matter **17**, L77 (2005).
- [25] M. Jaime *et al.*, Phys. Rev. Lett. **89**, 287201 (2002).
- [26] A.J. Legget *et al.*, Rev. Mod. Phys. **59**, 1 (1987).
- [27] J.R. Thompson *et al.*, Appl. Phys. Lett. **59**, 2612 (1991).
- [28] J.S. Kim *et al.*, Phys. Rev. B **67**, 014404 (2003).
- [29] V. Correa *et al.* (unpublished).
- [30] G. Blatter *et al.*, Rev. Mod. Phys. **66**, 1125 (1994).
- [31] T. Goto *et al.*, Physica B (Amsterdam) **346**, 150 (2004).